06

Shock-wave polymorphic transition in porous graphite

© S.A. Kinelovskii

Lavrentyev Institute of Hydrodynamics, Siberian Branch, Russian Academy of Sciences,
630090 Novosibirsk, Russia
e-mail: skineg41@gmail.com

Received May 10, 2021
Revised May 10, 2021
Accepted May 23, 2021

For the polymorphic transformation of porous graphite in the shock, the previously proposed model linking the process of graphite phase transition with a change in the elastic energy of a substance has been tested. It is shown that the model plausibly describes the experimental results outside the transition zone in a fairly wide range of changes in the porosity of samples with their different initial structure. It is discussed how the model under consideration changes the currently existing ideas about the thermodynamics of the polymorphic transition of matter in a shock wave.

Keywords: polymorphism, shock wave, porosity, graphite, diamond, phase transition.

DOI: 10.21883/TP.2022.14.55223.139-21

Introduction

The propagation of a shock wave through a crystalline substance can lead to a polymorphic transition i.e. rearrangement of the atomic structure of the substance. In [1] it is noted that „the formation of new crystalline modifications in short time intervals $\sim 10^{-7}$ s represents one of the most interesting subjects in shock wave physics and high pressure physics“.

The study of the graphite–diamond polymorphic transition has been intensively carried out for more than sixty years. Reviews of the results of these studies, in particular, can be found in the works [2–7]. Over the past years, a large amount of experimental data has been accumulated on the action of shock waves on graphite samples of various types and various porosity, but there is still no generally accepted model of the polymorphic transition of matter in a shock wave, the model that would describe the existing set of experimental data in a unified manner.

In the work [8], on the example of graphite, the model was proposed that relates the process of polymorphic transition in the shock wave to the change in the elastic energy of matter. There, this model was tried out for the case of almost non-porous pyrolytic graphite, since experimental data for solid graphite do not exist. In this work, the possibility of its applicability for pressed porous and other types of graphite in a fairly wide range of porosity values of the samples, is considered.

1. Problem formulation

To describe both phases of carbon, here, as in [8], the Mie-Gruneisen-type equations of state (EoS) are used in the form

$$p(\rho, T) = p_e(\rho) + p_h(\rho, T), \;\; p_h(\rho, T) = \Gamma_0 \rho E_{ih}(T),$$

$$E_{ih}(T) = c_v(T - T_0),$$

where the specific heat c_v and the Gruneisen coefficient Γ_0 are assumed to be constant; the temperature T_0 under normal conditions is assumed to be 300 K. The indices e and h correspond to the elastic and thermal components, and the index i corresponds to the internal energy.

The elastic components of pressure and energy are taken in the form

$$p_e = \frac{B_0}{n}\left(\left(\frac{\rho}{\rho_0}\right)^n - 1\right), \tag{1}$$

$$E_{ioe} = \frac{B_0}{n\rho_0}\left\{\frac{1}{n-1}\left[\left(\frac{\rho}{\rho_0}\right)^{n-1} - 1\right] + \left(\frac{\rho_0}{\rho} - 1\right)\right\}. \tag{2}$$

The parameters B_0 and n for graphite and diamond included in equations (1), (2) below will have indices g and d, respectively. Let's introduce the dimensionless temperature $\tau = T/T_0$, then the thermal components of pressure and energy take the form

$$p_h(\rho, \tau) = \Gamma_0 \rho \xi(\tau - 1), \quad E_{ih}(\tau) = \xi(\tau - 1), \tag{3}$$

where $\xi = c_v T_0$. Under initial conditions ($\rho = \rho_0$, $T = T_0$) all pressure and energy components are equal to zero. For entropy we derive the expression [9]

$$S = c_v \ln\left[\tau\left(\frac{\rho}{\rho_0}\right)^{\Gamma_0}\right]. \tag{4}$$

For the parameter points introduced above, values close to those used in the works [10,11]: $B_{0g} = 45$ GPa, $n_g = 5$, were taken: $\Gamma_{0g} = 0.3$, $B_{0d} = 420$ GPa, $n_d = 3.5$, $\Gamma_{0d} = 1$, $\rho_{0g} = 2.265$ g/cm^3 and $\rho_{0d} = 3.515$ g/cm^3, $c_{vg} = c_{vd} = 2$ kJ/(kg·K).

The experimental results will be used in the form „of the graphite branch“ of the Hugoniot's shock adiabat (SA) for velocities. These results will be approximated by linear dependences in the form $U_1(D) = a + \lambda D$, where a and λ are empirical coefficients, D is shock wave (SW) velocity, U_1 is mass velocity behind the SW front. As noted in [8], it is desirable to carry out the approximation in the SA region, near the beginning of the phase transition.

By means of the standard equations of dynamic compatibility at the front of shock wave propagating with a velocity D over material at rest, one can calculate the matter state behind the front:

$$\rho_1(D) = \frac{\rho_{0g} D}{D - U_1(D)}, \quad p_1(D) = \rho_{0g} D U_1(D), \qquad (5)$$

$$E_{i1}(D) = \frac{p_1(D)}{2}\left(\frac{1}{\rho_{0g}} - \frac{1}{\rho_1(D)}\right), \qquad (6)$$

where $U_1(D)$ is determined by the approximation introduced above, and the elastic component of the internal energy $E_{i1}(D)$ by formula (2). As a result, it is possible to determine the thermal component of internal energy, temperature, entropy and any other thermodynamic characteristics. The estimate of the graphite temperature at the SW front is carried out according to (3): $\tau_1(D) = 1 + E_{ihg1}/\xi$.

Further, according to [8], we assume that if the phase transition occurs at some point of the SA of graphite, then the density of the new phase is determined from the condition of equality of the elastic pressure components for both phases. Then the density $\rho_2(D)$ of the high-pressure phase is found from the equation following from (1):

$$\frac{B_{0g}}{n_g}\left(\left(\frac{\rho_1(D)}{\rho_{0g}}\right)^{n_g} - 1\right) = \frac{B_{0d}}{n_d}\left(\left(\frac{\rho_2(D)}{\rho_{0d}}\right)^{n_d} - 1\right). \qquad (7)$$

Equation (7) is used to determine only the value of the density $\rho_2(D)$ of the new phase. The resulting pressure differs from $p_1(D)$ due to the fact that when the crystal lattice is rearranged, the preserving condition of the flows of matter and ones of impulse are immediately violated and, as a result, the discontinuity appears in the values of the matter characteristics, i.e. shock wave appears. Since the second wave is inextricably linked with the first shock wave, and the process is assumed to be stationary, in the laboratory coordinate system the moving velocity of the second wave is also D, and in the system associated with the front of the first shock wave, this wave is motionless, which gives reason to call it as „phase jump“. Occurrence time of this wave is determined by the phase transformation duration and, according to experimental data, is $10^{-7}-10^{-8}$ s (see, for example, [11–15]). The density $\rho_2(D)$ of the material behind this wave is found from (7), the remaining flow characteristics are determined from the dynamic compatibility equations for this compression shock:

$$\rho_2(D) = \rho_{0d}\left\{\frac{B_{0g} n_d}{B_{0d} n_g}\left[\left(\frac{\rho_1(D)}{\rho_{0g}}\right)^{n_g} - 1\right] + 1\right\}^{1/n_d}, \qquad (8)$$

$$U_2(D) = D\left(1 - \frac{\rho_{0g}}{\rho_2(D)}\right),$$

$$p_2(D) = p_1(D) + \rho_{0g} D\big(U_2(D) - U_1(D)\big), \qquad (9)$$

$$E_{i2}(D) = E_{i1}(D) + \frac{p_1(D) + p_2(D)}{2}\left(\frac{1}{\rho_1(D)} - \frac{1}{\rho_2(D)}\right). \qquad (10)$$

Thus, all the characteristics of the high-pressure phase that are of interest to us have been determined. The temperature at the front of the second SW, like τ_1, is determined by the expression $\tau_2(D) = 1 + E_{ihd2}/\xi$. It should be immediately noted that, due to the assumptions made in the model about the form of the dependence $E_i(T)$ and the constancy of the values c_{vd} and Γ_d, the resulting value τ_2 in a greater degree than τ_1 should be considered as evaluative.

At the considered phase transformation, the elastic component of the energy decreases. Using (2) it is found that the decrease in the specific elastic energy in our case is determined by the expression $\Delta E_{e21}(D) = |E_{ied2}(D) - E_{ieg1}(D)|$. In [8] the condition for the complete transition of graphite to the diamond-like phase in the SW was formulated, which consists in the fact that this change must be greater than (or equal to) the specific work of the pressure applied to the medium p_1 by its additional compression:

$$\Delta E_{e21}(D) \geq \frac{1}{2} p_1(D)\left(\frac{1}{\rho_1(D)} - \frac{1}{\rho_2(D)}\right) = A_{21}. \qquad (11)$$

In this paper, the considered model is adapted to the case of a porous substance. The main problem that arises in this case is related to the fact that for a porous substance there is no EoS, the presence of which is provided for by the model. In this regard, in order to remain within the framework of the EoS considered above, to which the above calculations (in particular, formula (7)) correspond, we will use the approximation according to which the sample is considered to be continuous with reduced initial density (see, for example, [9]). Thus, we will assume that formulas (1)–(4) remain in force, and the elastic component of pressure of the porous substance is described (1) with the initial density $\rho_{00} = \rho_{0g}/m$ (i.e., the porosity m is determined as the ratio of the density of the continuous substance to the density of the porous one). The parameters B_0 and n can be considered as adjustable ones.

2. Study results

In this work, the data from known experiments with different sample porosities are used. All of them are mentioned in the experimental data base [16], where their primary sources are also indicated. Some of these data are shown in Fig. 1; the range of considered porosities is limited by the values $m = 1.03$ and 2.24; and recall that the first value refers to pyrolytic graphite. For graphite specimens with higher porosity, attention is not focused

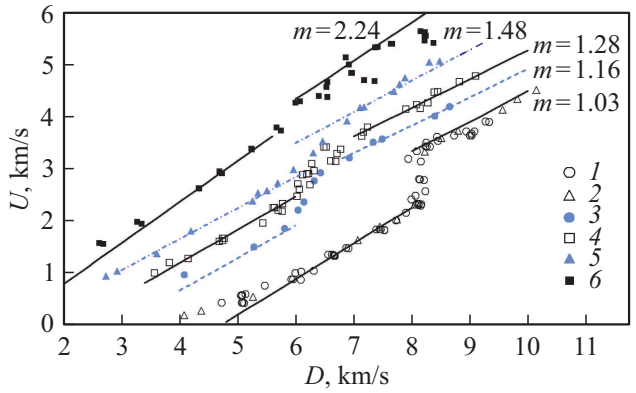

Figure 1. Calculated and experimental results for $(U\text{-}D)$−shock adiabat of graphite and diamond-like phase for different values of sample porosity. Calculation: SAs of graphite (left parts of the lines) and of diamond (right parts) for each porosity value. Dots are experimental data [16], m: *1* is 1.026, *2* is 1.029, *3* is 1.163, *4* is 1.28, *5* is 1.469, *6* is 2.24.

on the technology of their manufacture (pressed, glass-like, etc.), i.e. the attempt is made to consider them in the general group. It follows from the experimental data that for almost all porosities within the specified range, at SW velocity $D_1 \approx 6$ km/s, graphite phase transformation begins, and at $D_2 \approx 7$ km/s, it can be considered that all the graphite crossing the SW front completely transforms into the new phase. Thus, it is of interest to determine how the corresponding pressures p_{14} and p_{12} at the SW front depend on porosity, as well as the final pressure p_{22} at front of the phase jump corresponding to the velocity D_2.

We turn our attention to the choice of the values of model parameters. For the diamond-like phase, the values of the parameters remain unchanged, since it is logical to assume that the EoS of this phase should not depend on the initial state of the graphite sample. For porous graphite, in order to reduce the number of adjustable parameters, we assume that for all porosities $n = n_g$. Thus, only one adjustable parameter B_0 remains in the EoS, i.e.the analogue of volumetric modulus of elasticity for void-free material. The values of the other parameters introduced above for graphite are assumed to be unchanged. In addition, the model has two more parameters, a and λ are coefficients in the linear approximation of graphite SA, which was carried out by the least squares method. To a certain extent, these coefficients can also turn out to be adjustable, since, on the one hand, as noted above, we should approximate the SA segment immediately before the onset of the phase transition, and on the other hand, for some series of experiments in the specified SA segment, there are very few experimental points (up to two), so that the direct approximation, for example, by the least squares method, may give a dubious result. Finally, we have three adjustable parameters — B_0, a and λ. The adjusting results must satisfy the following conditions:

1. The calculated curve $U_2(D)$ („diamond“ segment of SA) must describe the experimental data.

2. The calculation of the moment when all graphite passes into the diamond-like phase (i.e. condition (11) with the equal sign) must correspond to the experiment.

3. The obtained dependences of the parameters $B_0(m)$, $a(m)$ and $\lambda(m)$, as well as some characteristics of the process (for example, the pressure of the beginning of the phase transformation, etc.) would be, as possible, sufficiently smooth functions of m.

Analysis of the performed calculations showed that the values of the parameters that ensure the fulfillment of all three conditions lie in rather narrow ranges of their variation. The values of parameters of porous graphite samples accepted as a result are given in Table 1. Note that the data given for $m = 1.03$ is slightly different from [8]. On the one hand, they were obtained there at $B_0 = 45$ GPa. On the other hand, we conditionally assume here that this value should correspond to non-porous graphite $(m = 1)$, and therefore the simulation was carried out with a slightly lower value B_0, provided that the three conditions formulated above are met. Practically for all variants of m correction of the coefficients a and λ was not required, since there were a sufficient number of points for graphite SA, but in specific cases the correction turned out to be necessary. For example, Fig. 2 shows the case for $m = 1.06$, when there are only two experimental points for the SA graphite branch. Figure 3 shows the $\Delta E_{e21}(D)$ and $A_{21}(D)$ dependences obtained as a result of calculations using the adjustable approximation of the SA graphite branch. At the same time, if we were to use the SA approximation in the form of a straight line passing through these two points (line *3* in Fig. 2), then the curves shown in Fig. 3 would not intersect at all. Also, for $m = 1.518$, the noticeable correction of the approximation was required, due to the scatter of experimental data. In addition, in two more cases ($m = 1.05$ and 1.118), a very small correction of these parameters was required to ensure the simultaneous fulfillment of the above fitting conditions.

Table 1. Values of model parameters

m [16]	Type of graphite	ρ_{00}, g/cm^3	B_0, GPa	$-a$, km/s	λ
1.026	Pyrolytic	2.21	44	3.013	0.654
1.029	Pyrolytic	2.2	43	2.72	0.62
∼ 1.05	Ceylon, pressed	2.157	36	1.638	0.505
1.06	Pressed	2.133	30	1.98	0.568
1.118	Pressed	2.03	20	1.67	0.56
1.163	of ZTA brand	1.95	16.5	1.085	0.497
1.206	Pressed	1.87	7.8	1.256	0.574
1.21	Reactor				
1.280	Pressed	1.77	6	1.125	0.584
1.48	3D fiber	1.53	2.8	0.751	0.602
1.518	Glass-like	1.492	2.2	1.594	0.742
2.240	Pressed	1.01	0.2	0.541	0.752

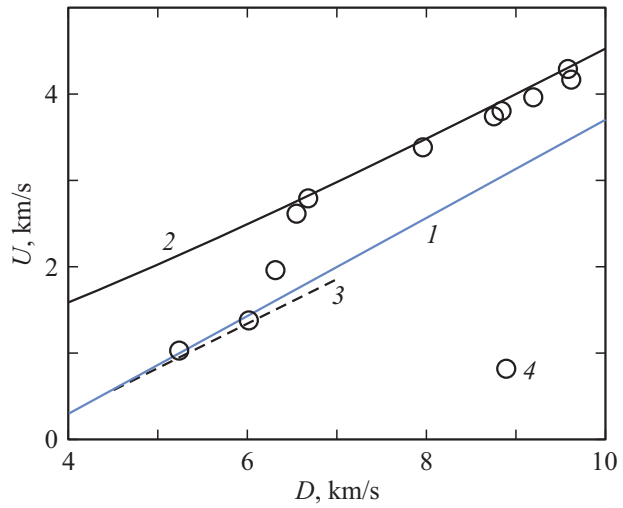

Figure 2. Shock adiabat for $m = 1.06$. Lines: *1* is graphite branch obtained as a result of fitting, *2* is calculated diamond branch, *3* is graphite branch approximation by two experimental points. Dots: *4* are experimental data [16] for $m = 1.061$.

Table 2. Values of the characteristic quantities of the process of polymorphic transformation of porous graphite

m	D_1, km/s	D_2, km/s	p_{14}, GPa	τ_{14}	p_{12}, GPa	τ_{12}	p_{22}, GPa	τ_{22}
1.03	8	8.2	39.2	2.5	42.6	2.7	62.3	12.0
1.05	6.5	7	23.1	1.6	28.6	2.0	44.6	8.9
1.06	6.2	7	20.4	1.7	29.8	2.3	43.2	9.4
1.118	6	7	20.5	2.0	31.9	3.2	44.9	11.3
1.163	6	7	22.2	2.4	32.7	3.7	45.2	12.5
1.21	6	7	24.5	3.7	36.1	5.7	44.7	15.3
1.280	6	7	25.1	4.3	36.5	6.5	44.7	17.3
1.48	6	7	26.3	6.2	35.9	9.1	42.3	22.7
1.518	6	6.8	25.6	6.5	35.0	9.2	41.9	24.1
2.240	5.5	6	20	10.7	25.8	13	27.9	28.4

Some results of calculations using formulas (5)–(10) for $(U-D)$–SA are presented in Fig. 1 for the porosity values indicated there. The complete results of calculations for various m in the form of values of the characteristics of the medium of interest to us are presented in Table 2. Here the designations are used: D_1 — SW velocity at which the phase transition begins; D_2 is SW velocity at which all graphite crossing the front passes into the new phase; $p_{14} = p_1(D_1)$, $\tau_{14} = \tau_1(D_1)$, $p_{12} = p_1(D_2)$, $\tau_{12} = \tau_1(D_2)$, $p_{22} = p_2(D_2)$, $\tau_{22} = \tau_2(D_2)$.

It can be seen from the data in Table 1 that, contrary to condition 3, it is not possible to ensure the smoothness of the functions $a(m)$ and $\lambda(m)$. This is mainly due to the alternation of graphite types, which leads to abrupt jumps in their value, while this is not observed for other characteristics.

Figure 4 shows the most interesting characteristic quantities: the dependence of the coefficient in the EoS $B_0(m)$ obtained as a result of modeling and the dependences $p_{14}(m)$ and $p_{12}(m)$, and the last two were obtained from the processing of the used experimental data [16] and are actually not related to the model under consideration. In addition, the diagram additionally presents data from works [5,13,17,18]. In particular, the point [17] with the porosity $m \approx 1.015$ is slightly shifted to the right so that it is not cut off by the axis. In the region of the local minimum $p_{14}(m)$ $(m = 1.05-1.1)$, in addition to the point shown [13], there are data practically coinciding with it from the papers [7,17,19] (not shown on the chart).

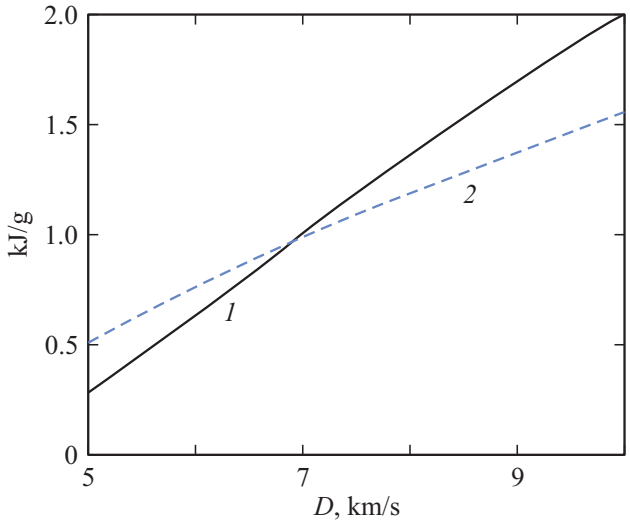

Figure 3. Calculated dependences for $m = 1.06$: *1* for specific elastic energy released during the phase transition, *2* for specific work required for additional compression of the substance during this transition.

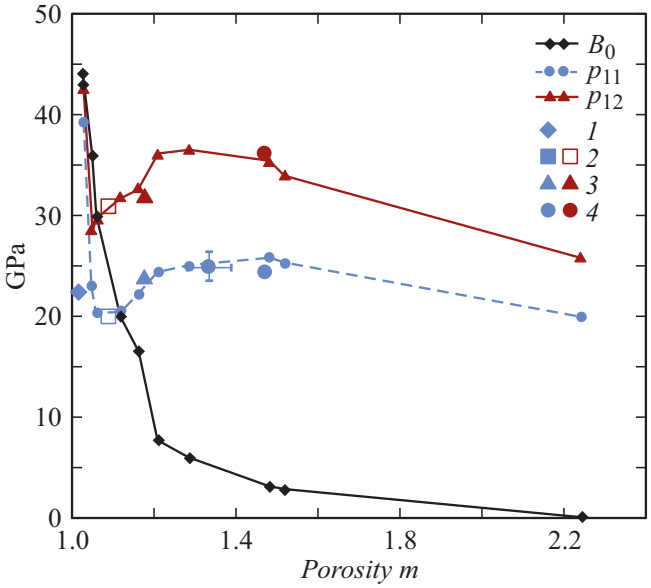

Figure 4. Dependences of the EoS parameter B_0 and the characteristic pressures p_{14} and p_{12} on porosity (lines). Experimental data: *1* — [17], *2* — [13], *3* — [5], *4* — [18].

In Fig. 5, in comparison with the experiment, the calculated results for $(U-D)$–SA for the case $m = 1.21$, where the approximation parameters a and λ exactly correspond to results defined by the method of least squares, are presented. Experimental data [16] refer to two variants of graphite with close values m.

In Fig. 6 for the same porosity value, the calculated graphite and diamond branches $(p\text{-}V)$–SA are presented in comparison with the data from the database [16] It should be noted that these are not exactly the SAs of graphite and diamond, since they are obtained on the basis of the applied linear approximation $U_1(D)$. This, in particular, is indicated by a slight deviation of the curve for graphite from the data [16] at low pressure. In addition, the diagram shows wave rays emerging from the point of the initial state of the sample material and corresponding to SW velocities D_1 and D_2 from Table 2.

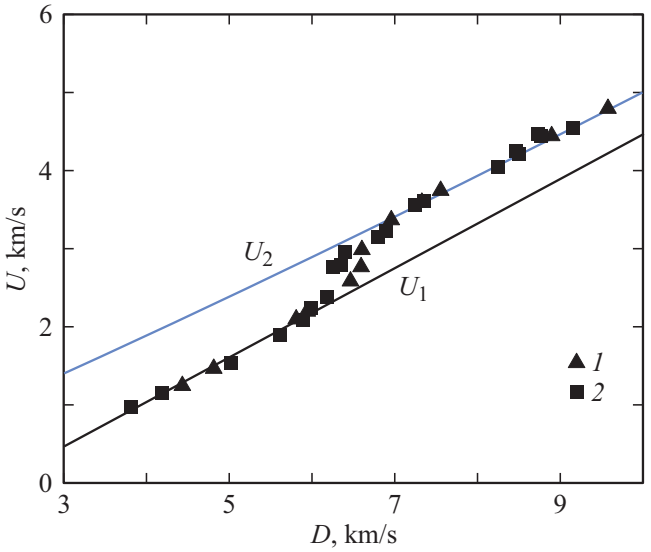

Figure 5. Calculated and experimental results for $(U\text{-}D)$–SA of graphite and diamond-like phase at $m = 1.21$. Lines: U_1 are graphite branch and U_2 diamond one of SA. Experiment [16]: *1* is $m = 1.21$, reactor graphite; *2* is $m = 1.206$, pressed graphite.

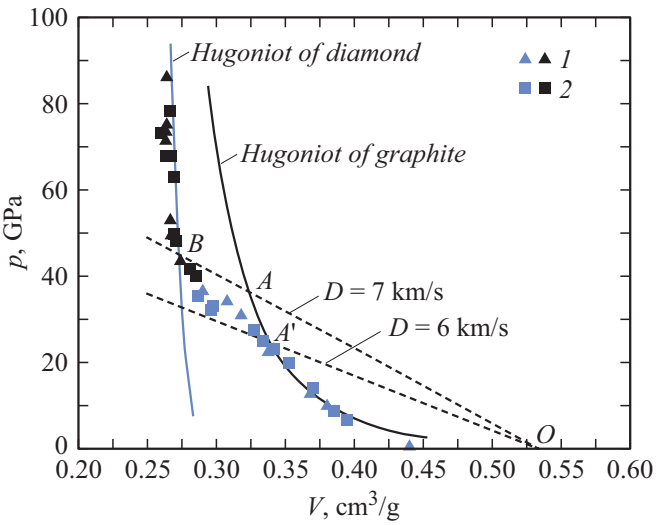

Figure 6. Calculated (solid lines) and experimental (dots) results for $(p\text{-}V)$–SA graphite and diamond-like phase at $m = 1.21$. Dashed lines are wave rays for two values of SW velocity. Experiment [16]: *1* — $m = 1.21$, reactor graphite; *2* — $m = 1.206$, pressed graphite.

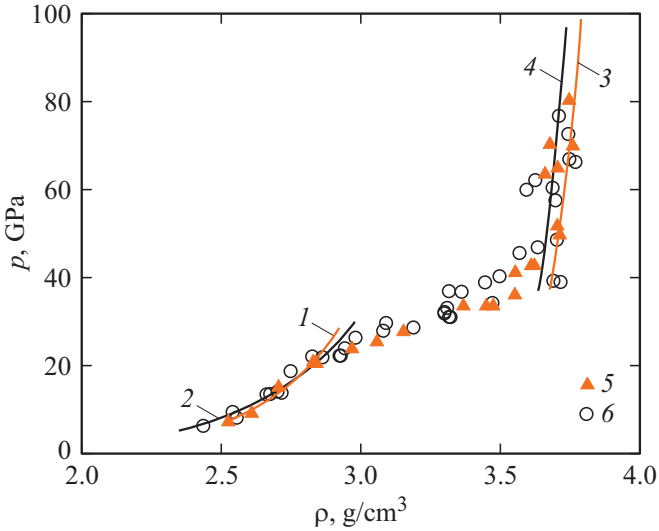

Figure 7. Calculated (lines) and experimental (dots) results for $(p\text{-}\rho)$–SA graphite and diamond-like phase. Calculation: *1, 2* — SA for graphite; *3, 4* — SA for diamond; *1, 3* — $m = 1.16$; *2, 4* — $m = 1.28$. Experiment: *5* — $m = 1.163$, *6* — $m = 1.280$.

Figure 7 shows the calculated $(p\text{-}\rho)$–SA for two porosity values in comparison with the data from the [16] database. It should be immediately noted that the data [16] shown in the last two diagrams can only be called as deemeded experimental data, since in all databases they are calculated using formulas (5), where U is measured in experiment, i.e. by compression in one SW. The point is that for the transition region for the diamond branch of the SA, compression actually occurs sequentially in two SWs, and one can only assume that at sufficiently high SW velocities, one SW will again remain. Therefore, on some part of the SA, these data do not correspond to reality and can be considered as estimated ones.

3. Discussion of results

First we turn our attention on the results presented in Table 2. It is important, in the author's opinion, that with the same chemical composition, but different structure of the sample material, all the results were described within the framework of one model. This means that at the level of load that is achieved with shock wave action, the structure of the material (recall that we considered pressed materials from graphite powders of various origins and various degrees of grinding, artificial and vitreous graphite, as well as pressed fibers) is not particularly important, and modeling can be carried out only by the density of the

material. In particular, this is of interest for the development of optimal modes for the shock-wave synthesis of diamond powders.

The maximum allowable porosity is apparently $m \approx 2$, since for $m = 2.24$ (Fig. 1) the phase transition occurs at $D \approx 6$ km/s, and already at $D > 6$ km/s, the chaotic expansion of the material occurs. The temperature estimate (Table 2) in this case gives $T_2 > 8000^\circ$C, which is sufficient for the manifestation of various effects (for example, partial graphitization, material melting, etc.).

According to Fig. 4, simulation for $B_0(m)$ gave a fairly smooth function, and processing of experimental data [16] for p_{14} showed that the function $p_{14}(m)$ is not smooth, and this is also confirmed by data from other papers. For now, the sharp drop of the value of p_{14} during the transition from pyrolytic graphite ($m = 1.03$, $p_{14} \approx 42$ GPa) to porous pressed graphite with $m = 1.05$ ($p_{14} \approx 20$ GPa) [8,16] and the presence of a local minimum at $m = 1.06-1.10$, inexplicable from a physical point of view. In particular, this drop cannot be fully explained by noted in [7] „the decrease in the transformation pressure with an increase in the degree of graphite order". Recall that this conclusion was made on the basis of experiments with samples of different types of graphite in the porosity range $m = 1.02-1.11$, in which the pressure of the beginning of the transformation varied in the range $p_{14} \approx 23-19$ GPa. At the same time, it is not commented there that at $m = 1.01-1.03$ for pyrolytic graphite $p_{14} > 40$ GPa

As for the above local minimum, the subsequent slight increase in p_{14} is confirmed, in addition to [16], as mentioned above, also by the results of other studies. The temperature values given in Table 2, which are given by the calculation model at the front of the first SW at the beginning of the phase transition in the region of the local minimum $p_{14}(m)$, practically coincide with the results [7], where they were obtained from calculations according the wide-range EoS of graphite.

One more point can be noted, which follows from the simulation (Table 2): in the range of porosity values $m = 1.06-1.50$, the pressure p_{22} after the phase transition changes slightly and close to the value B_0 for pyrolytic graphite.

The results of the performed simulation show (Fig. 1, 2 and 5) that, as in [8], the model quite well describes the mass velocity $U_2(D)$ of medium after the phase transition. In this case, under the assumption that the graphite SA remains the straight line, both branches of the SA gradually approach each other with increase in SW velocity, i.e. the intensity of the phase jump decreases. In the limit for very large values D ($\sim 30-50$ km/s) these lines become parallel. This means that the considered phase transition never occurs in one SW. To tell the truth, for $m = 2.24$ it was found that at $D \approx 25$ km/s both lines merge into one. Perhaps this is a consequence of the not very good approximation of the SA of graphite.

The fact that the model describes the mass velocity $U_2(D)$ gives grounds to assume that the other thermodynamic characteristics of the medium are also plausibly described within the framework of the defined EoS, since all of them are calculated according to the conservation laws. The key factor of the model is equation (7), which makes it possible to immediately determine the density ρ_2 of the new phase during the phase transformation, which corresponds to the elastic component of the pressure at the front of the first SW. On the one hand, this is justified for sufficiently weak shock waves, since the thermal effects are small in this case. However, in [8] it was shown that for $m = 1.03$ the model quite accurately describes the experimental data [20] for U_2 at very large values D (note that U_2 and ρ_2 are uniquely related by the mass flux conservation equation at the SW front) when the thermal components in the characteristics of the medium are already large. In addition, for this case, calculations were also carried out, when an equality analogous to (7) is written for the total pressure. In this case, it turned out that in this case the calculated values U_2 quite significantly cease to correspond to the experimental results (it should be noted that all this was obtained within the framework of the accepted EoS).

For low-porosity ($m \leq 1.03$) graphite, the model completely describes the state of the diamond-like phase after the phase transition. For the porous substance, the model predicts the SW velocity D_2, at which the entire material crossing the SW front will pass into the new phase. In this case, the phase transformation always occurs in a system of two waves — the first SW and a phase jump, which has the same speed D in the laboratory coordinate system, and the intensity of this jump decreases with increasing SW speed. At the SW velocity in the range $D_1 < D < D_2$, as follows from the experiment, there is a region of incomplete transition of the substance or, as it is often called, a „region of mixing of two phases". In such a region, the state of substance becomes non-equilibrium, which makes it impossible to use the model under consideration. The author intends to consider the possibility of describing the process in this region in the next work.

Nonetheless even now, one can try to evaluate how the model under consideration changes the currently existing ideas about the thermodynamics of polymorphic transition in SW. Recall that these representations were based on the concept of system stability in our case of two SWs (see, for example, [1,2]). We will carry out the consideration, as is the convention, on the plane (p, V) using the example of Fig. 6. For the case of the void-free material (then in Fig. 6 there is no wave beam corresponding to a lower velocity D_1), point A corresponds to the state at the front of the first SW. According to existing concepts, at the point A, the SWs splits into two ones and the transition to the state $p_A < p < p_B$ on the shock adiabat of the second phase (this is the curve passing through the experimental points) is carried out using the second SW. Based on the concept mentioned above, this wave configuration will be stable if (see, for example, [2]) the inequation is realized,

$$\frac{p_2 - p_1}{V_1 - V_2} < \frac{p_1}{V_0 - V_1}, \tag{12}$$

which is written here in terms of the present work. Since it is realized in our case, this justifies the stratification of the first SW. For states on the shock adiabat of the second phase $p > p_B$, inequation (12) changes sign, and only one SW will be stable. From here it is concluded that, starting from the point B, the final state is reached in one SW. Nothing fundamentally changes in the case considered in this work, when the phase transition begins at $p < p_A$. Then the second wave ray OA' appears in Fig. 6, and all conclusions remain the same.

In the model under consideration, the fundamental difference is that all states on the SA of the new phase, which lie above the point B, are achieved as a result of the successive action of two SWs for any (within reasonable limits) values D. Another difference is that on any wave ray drawn from the initial state O and passing above the ray OAB (Fig. 6), using equation (7), one can indicate the point corresponding to the state of the new phase . In this case, the question of the stability of the wave configuration does not arise, since for all points of the SA expression (12) is an equation (note that this was expected, since the pattern is stationary in the SW system).

Conclusion

The work shows, that the model linking the process of polymorphic transformation of graphite into hydrocarbons with a change in the elastic energy of a substance can be quite successfully used in cases where the loaded samples are porous and have different initial structures. Estimates are obtained for the main thermodynamic quantities characterizing the polymorphic transition, depending on the porosity of the samples. It is shown that additional compression of substance to the density of the new phase occurs in a phase jump that occurs behind the SW front and has the same velocity in the laboratory coordinate system.

The model does not describe the process in the region of incomplete transformation of the substance, but this does not prevent us from obtaining some estimates of how it changes the currently existing ideas about the thermodynamics of polymorphic transition in hydrocarbons.

Conflict of interest

The author declares that he has no conflict of interest.

References

[1] L.V. Al'tshuler. J. Appl. Mech. Tech. Phys., **19** (4), 496 (1978).
[2] G.E. Duvall, R.A. Graham. Rev. Modern Phys., **49** (3), 523 (1977). DOI: 10.1103/RevModPhys.49.523
[3] F.P. Bundy, W.A. Basset, M.S. Weathers, R.J. Hemley, H.U. Mao, A.F. Goncharov. Carbon., **34** (2), 141 (1996). DOI: 10.1016/0008-6223(96)00170-4
[4] A.V. Kurdyumov, A.N. Pilyankevich. *Fazovyye prevrashcheniya v uglerode i nitride bora* (Naukova dumka, Kiyev, 1979) (in Russan)
[5] A.Z. Zhuk, A.V. Ivanov, G.I. Kanel'. High Temperature, **29** (3), 380 (1991).
[6] A.B. Kurdyumov, V.F. Britun, N.I. Borimerchuk, V.V. Yarosh. *Martensitnyye i diffuzionnyye prevrashcheniya v uglerode i nitride bora pri udarnom szhatii* (Izd-vo Kupriyanova, Kiyev, 2005) (in Russan)
[7] G.I. Kanel', G.S. Bezruchko, A.S. Savinykh, S.V. Razorenov, V.V. Milyavskii, K.V. Khishchenko. High Temperature, **48** (6), 806 (2010).
[8] S.A. Kinelovskii. J. Appl. Mechan. Tech. Phys., **61** (4), 623 (2020). DOI: 10.1134/S0021894420040161
[9] Ya.B. Zel'dovich, Yu.P. Raizer, *Fizika udarnykh voln i vysokotemperaturnykh gidrodinamicheskikh yavlenii* (Nauka, M., 1966) (in Russian).
[10] V.B. Rozanov, M.A. Rumyantseva. In coll.: *Kratkiye soobshcheniya po fizike FIAN*. **3/4**, 9 (1997) (in Russian).
[14] V.V. Prut. Tech. Phys., **62** (5), 720 (2017). DOI: 10.1134/S1063784217050231
[12] A.V. Ananyin, A.N. Dremin, G.I. Kanel, S.V. Pershin. PMTF, **3**, 112 (1978) (in Russian).
[13] M.F. Gogulya, D.G. Batukhtin, I.M. Voskoboinikov. Pis'ma v ZhTF, **13** (13), 786 (1987) (in Russian).
[14] M.N. Kravchenko. In coll.: *Issledovaniye svoystv veshchestva v ekstremal'nykh usloviyakh* (In-t vysokikh temperatur AN SSSR, M., 1990) (in Russian)
[15] D.J. Erskine, W.J. Nellis. J. Appl. Phys., **71** (10), 4882 (1992).
[16] Electronic database of shock-wave experiments. Electronic source. Available at: http://www.ihed.ras.ru/rusbank/catsearch.php
[17] A.S. Savinykh, G.I. Kanel, S.V. Razorenov. Physics Solid State, **49** (11), 2185 (2007).
[18] W.H. Gust. Phys. Rev. B, **22** (10), 4744 (1980).
[19] G.S. Bezruchko, G.I. Kanel', S.V. Razorenov, A.S. Savinykh, V.V. Milyavskii. JETP Lett., **88** (3), 220 (2008).
[20] W.J. Nellis, A.C. Mitchell, A.K. McMahan. J. Appl. Phys., **90** (2), 696 (2001).